

Thermal Creation of Electron Spin Polarization in n-Type Silicon

André Dankert^{1, a)} and Saroj P. Dash^{1, b)}

Department of Microtechnology and Nanoscience, Chalmers University of Technology, SE-41296, Göteborg, Sweden

Conversion of heat into a spin-current in electron doped silicon can offer a promising path for spin-caloritronics. Here we create an electron spin polarization in the conduction band of n-type silicon by producing a temperature gradient across a ferromagnetic tunnel contact. The substrate heating experiments induce a large spin signal of $95 \mu\text{V}$, corresponding to 0.54 meV spin-splitting in the conduction band of n-type silicon by Seebeck spin tunneling mechanism. The thermal origin of the spin injection has been confirmed by the quadratic scaling of the spin signal with the Joule heating current and linear dependence with the heating power.

Keywords: Silicon, Hanle, Three-Terminal, Thermal Spin Injection, Spin Seebeck Effect

Ultra large scale integration and miniaturization of electronic devices and circuitry yield to an increase in Joule heat dissipation and wastage of energy. An effort to reduce, reuse or redirect this heat is not only of technological, but also has fundamental and ecological importance. In this regard caloritronics explores the possibility of directly converting heat into electricity¹. On the other hand spintronics offers a promising path to achieve lower energy consumption^{2,3}. An exciting new research field taking advantage of both of these areas, called spin-caloritronics, is attracting a growing interest^{4,5}. Recently, many physical phenomena connecting spin to thermal effects have been proposed and demonstrated such as spin-Seebeck effect⁶, spin dependent Seebeck effect in nanostructures and thermal spin injection into metal⁷, thermal spin-transfer torque^{8,9}, spin-related Peltier cooling¹⁰, and thermal spin tunnel effects^{11,12}. Especially interesting is the Seebeck spin tunneling into semiconductors, which is sensitive to the energy derivative of tunnel spin polarization at the interfaces¹².

The strong interest in Si for spintronics stems from its long spin coherence length, caused by the absence of hyperfine interactions and a weak spin-orbit coupling, and its industrial dominance^{13,14}. Recently, electrical spin polarization in Si could be created at room temperature by spin polarized tunneling from a ferromagnet (FM)¹⁵⁻¹⁹. The Hanle and the inverse of the Hanle effects were used for the detection of spin polarization in different semiconductors under ferromagnetic tunnel contacts²⁰. Using such Hanle techniques, Le Breton et al. demonstrated a spin accumulation in hole doped p-type Si by using the Seebeck spin tunneling mechanism¹². In a FM/tunnel barrier/semiconductor structure, a temperature difference between the electrodes creates a tunnel spin current^{12,21-23}, which is governed by the energy derivative of the tunnel spin polarization (TSP). This involves thermal transfer of spin angular momentum from the ferromagnet to Si without net tunneling charge cur-

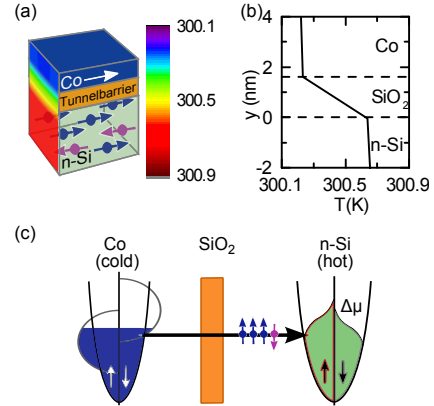


Figure 1. **(Color online)** (a) Device structure and simulated temperature distribution across the Co/SiO₂/n-type Si. (b) Temperature line scan across the tunnel contact for 1.5 nm thick SiO₂ at heating current 20 kAcm^{-2} . (c) Spin-dependent density of states and its occupation for a tunnel contact with a hot Si and a cold Co electrode. The different energy dependence of tunnel spin polarization for forward and reverse tunneling process gives rise to a finite spin current, without any net charge current.

rent. For Si based devices, these experiments are yet limited to reports on hole doped p-type Si with Al₂O₃ / NiFe tunnel contacts¹². For further development, it is required to have spin tunnel contacts with strong variation in TSP around the Fermi energy (EF), tunnel barriers with high interface thermal resistances, and its implementation in both electron and hole doped Si¹². Therefore, a detailed investigation of spin Seebeck tunneling effect with new ferromagnetic tunnel contact materials, and electron doped n-type Si is crucial from fundamental and technological point of view.

In this letter, we report a thermal creation of electron spin polarization in n-type Si by using the Seebeck spin tunneling mechanism. The temperature gradient between the n-type Si substrate and the FM yields to Seebeck spin tunnel currents, creating a large spin accumulation in the Si conduction band. We particularly use ferromagnetic tunnel contacts with ozone oxidized SiO₂

^{a)}Electronic mail: andre.dankert@chalmers.se

^{b)}Electronic mail: saroj.dash@chalmers.se

tunnel barriers and Co ferromagnet on heavily doped n-type Si. The detection of this thermally induced spin polarization was performed by employing Hanle and inverted Hanle effects in four-terminal measurement geometry. The amplitude of the thermal spin signal scales quadratically with the Joule heating current density and linearly with the heating power, which confirms the thermal origin of the observed Hanle signal. Electrical measurements and high magnetic field experiments rule out any other type of thermomagnetic effects. This result offers a way to generate a large electron spin accumulation in n-type Si by thermal spin injection using Seebeck spin tunneling.

For thermal spin injection into the n-type Si (measured electron density of $3 \cdot 10^{19} \text{ cm}^{-3}$ at 300 K) FM tunnel contacts (Co/SiO₂) were fabricated on initially patterned $2 \mu\text{m}$ thick silicon-on-insulator (SOI) channels (with the dimensions $200 \times 1000 \mu\text{m}^2$). The SiO₂ tunnel barrier was formed on the Si by ozone oxidation at room temperature. The chips were exposed to O₃, created by a constant O₂ flow (11/min) in the presence of a UV radiation source. This process results in uniform and pinhole-free tunnel barriers of 1.5 nm thickness. This is confirmed by the temperature and thickness dependent measurements of the junction resistance²⁴. Using such SiO₂ tunnel barrier, a very large spin polarization in silicon could be achieved by electrical method²⁴. After oxidation the samples were transferred to an electron beam deposition system, where 15 nm Co and 10 nm Au were deposited. The FM contacts were patterned by photolithography and Ar-ion beam etching. Subsequently, Cr (10 nm)/Au (100 nm) contacts on the Si, and contact pads on the ferromagnetic tunnel contacts were prepared by photolithography and lift-off technique. The Cr/Au contacts were used for the Joule heating of the Si and as reference contacts to detect a voltage signal with respect to the FM tunnel contact. The ferromagnetic tunnel contacts have an area of $200 \times 100 \mu\text{m}^2$ allowing a sufficiently good signal-to-noise ratio.

The principle for the thermal creation of spin accumulation in Si using the Seebeck spin tunneling mechanism is illustrated in Fig. 1. The simulated temperature distribution across the interface of the Co/SiO₂ (1.5 nm)/n-type Si device is shown in Fig. 1a and b. The complete device structure of Au (100 nm)/Co (15 nm)/SiO₂ (1.5 nm)/n-type Si ($2 \mu\text{m}$) were considered for our calculation. A model was drawn to scale with our device and divided into finite elements using commercial software (COMSOL) for calculating their temperatures. The temperature gradient (ΔT) is created by dissipation of an applied current density of 20 kAcm^{-2} . The simulation takes Joule heating due to current flow and heat dissipation, transport and radiation into account with a base temperature of 300 K. Here we have used a heat conductance $k_{\text{SiO}_2} = 0.95 \text{ Wm}^{-1}\text{K}^{-1}$ for thin SiO₂ tunnel barriers²⁵. Taking the large thermal conductivity of the Au pads and wire bonding into account, the surface temperature of the contact pads was fixed to 300 K. This

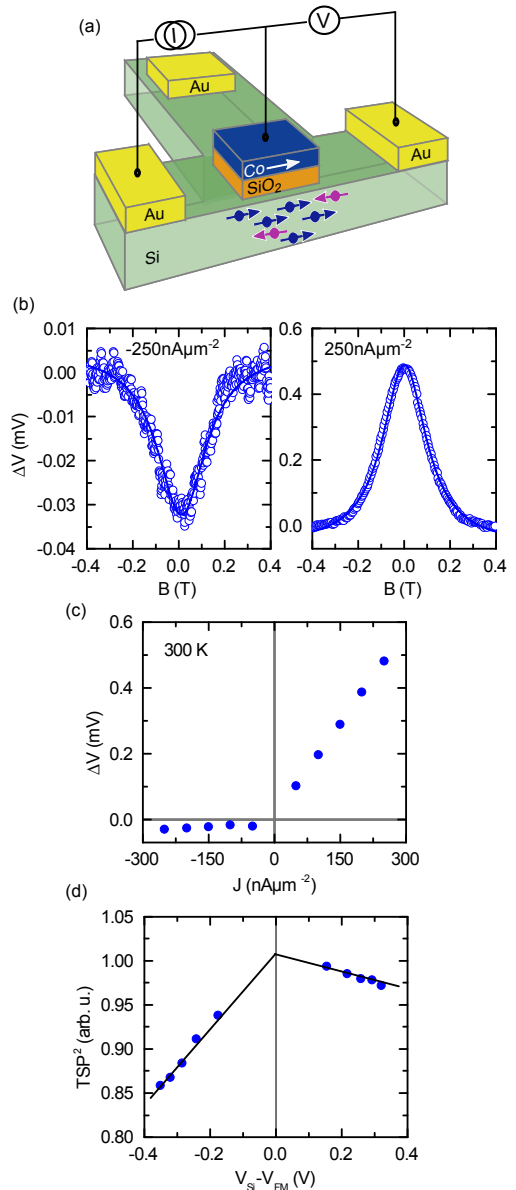


Figure 2. **(Color online) Electrical Hanle effect at room temperature.** (a) Three-terminal Hanle geometry for electrical injection and detection of spin polarization in the n-type Si with a SiO₂-Co tunnel contact. (b) The electrical detection of spin polarizations in n-type Si at 300 K by Hanle effect for spin injection ($I = +250 \text{ nA} \mu\text{m}^{-2}$) and spin extraction ($I = -250 \text{ nA} \mu\text{m}^{-2}$). The solid lines are the Lorentzian fits with lower limit for spin life time $\tau_{sf} = 50 \text{ ps}$. (c) Electrical bias current dependence of the Hanle voltage signal (ΔV). (d) Electrical bias voltage dependence of TSP^2 , which is proportional to the Spin-RA of the detected Hanle signal.

results in a temperature gradient $\Delta T = 500 \text{ mK}$ between the Si (T_{Si}) and Co (T_{FM}). Such temperature difference yields to a nonequilibrium electron distributions in the Co and Si near the Fermi energy. This results in tunneling of equal number of electrons in opposite directions, giving rise to a zero net charge current. However, as

the energy dependence of TSP is known to be different for the forward and reverse tunneling processes^{26,27}, a spin accumulation ($\Delta\mu$) can be induced in the Si (Fig. 1c)^{12,21}.

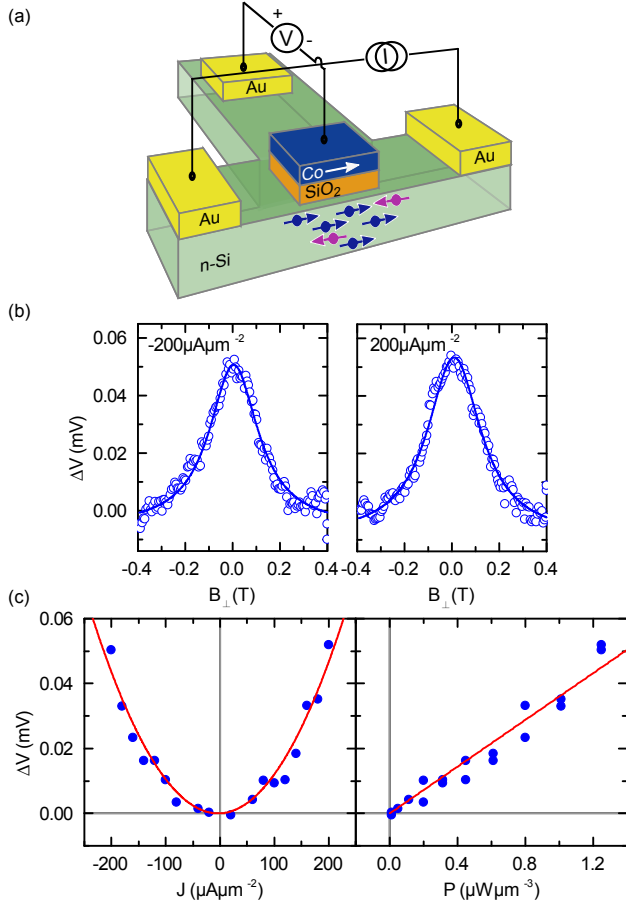


Figure 3. **(Color online) Thermal Hanle effect at room temperature.** (a) Device geometry and measurement scheme showing the Si Joule heating by a DC current, resulting in $T_{Si} > T_{FM}$. The voltage across the ferromagnetic tunnel contact is measured, with reference to another Cr/Au contact placed on Si. (b) Thermally induced spin accumulation in Si, detected as a voltage change (ΔV) by the Hanle effect with perpendicular magnetic field. The plots show the data for heating current in two opposite directions ($\pm 200 \mu A \mu m^{-2}$) at 300 K. The solid lines are Lorentzian fits to the Hanle curves. (c) Left panel: Thermal Hanle signal ΔV (symbols) versus Joule heating current density, with a quadratic fit (solid line). Right panel: ΔV (symbols) as a function of Joule heating power, and a linear fit (solid line).

Before performing thermal spin injection experiments we have tested the contacts for electrical spin injection and verified the energy or bias dependence of TSP . The measurements were performed in a three-terminal Hanle geometry as shown in Fig. 2a. Electrical spin injection creates a majority spin accumulation and splitting of the electrochemical potential in the conduction band of the Si. The Hanle effect is used for the controlled reduction of the induced spin accumulation by applying a magnetic

field (B_{\perp}) perpendicular to the FM magnetization direction. The spin accumulation decays as a function of B_{\perp} with an approximately Lorentzian line shape given by $\Delta\mu(B_{\perp})$, where $\Delta\mu(0)$ and $\Delta\mu(B_{\perp})$ are the spin accumulations in zero and finite perpendicular magnetic field, respectively, and τ_{sf} is the lower limit for spin lifetime^{15,24}. Figure 2b shows the measurement of the electrical Hanle signal for bias currents of $\pm 250 nA \mu m^{-2}$ (corresponding bias voltage of $\pm 300 mV$) at 300 K. The spin injection ($V_{Si} - V_{FM} > 0$) from the Co/SiO₂ tunnel contact creates a majority spin ($n \uparrow$) accumulation, whereas the spin extraction ($V_{Si} - V_{FM} < 0$) creates a minority spin ($n \downarrow$) accumulation in the Si. As expected the measured Hanle signal for majority and minority spin accumulation are found to be of opposite sign. The spin accumulation $\Delta\tau$ scales with the tunnel spin polarization (TSP) of the injected current and with spin life time (τ_{sf}). The detected voltage due to spin accumulation can be written as $\Delta V = TSP \cdot \frac{\Delta\mu}{2}$. This results in the detected spin signal (spin resistance area product, spin-RA) which is proportional to $TSP^2 \cdot \tau_{sf}$. The variation of TSP^2 vs. bias voltage is presented in Fig 2d and is found to be asymmetric. The strong decay of TSP^2 for energies above E_F ($V_{Si} - V_{FM} < 0$) results in the direction dependent spin polarized tunnel currents^{12,21}. The difference in spin polarization of the currents tunneling into and out of the Si can yield to a spin injection in our Co/SiO₂/n-type Si devices^{12,26,27}. This asymmetry in the TSP^2 of Co/SiO₂/n-type Si contact is essential to induce the large thermal spin accumulation in Si via Seebeck spin tunneling mechanism.

The thermally induced electron spin accumulation in n-type Si has been created by introducing a temperature gradient between the Si (T_{Si}) and Co (T_{FM}) separated by a thin SiO₂ tunnel barrier (1.5 nm). We increase the temperature of Si channel (T_{Si}) by a DC current due to Joule heating. The SiO₂ tunnel barrier prevents the current and heat from spreading into the ferromagnetic electrode. The temperature gradient created across the SiO₂ barrier ($T_{Si} > T_{FM}$) results in spin polarized Seebeck tunnelling through the oxide barrier, since the TSP for ingoing and outgoing currents differs. This creates a spin accumulation in the Si conduction band and therefore a splitting of the electrochemical potential ($\Delta\mu$) as shown in Fig 1c. The detection of a thermally induced spin accumulation in Si is performed in both Hanle and inverted Hanle geometry using a SiO₂/Co contact^{12,15}. A voltage signal is detected while sweeping a magnetic field, under the condition of zero net tunnel charge current ($I_{tunnel} = 0$) between the Co and the Si^{12,15}.

A significant thermal Hanle spin accumulation signal of $\Delta V_H = 50 \mu V$ is observed in the Si for $T_{Si} > T_{FM}$, for a Joule heating current density of $J = \pm 200 \mu A \mu m^{-2}$ (Fig. 3b). The Lorentzian line shape of the thermal Hanle signal obtained here is consistent with our electrical Hanle measurements. The magnitude and sign of the thermal Hanle curves are also identical for both directions of the Joule heating current. This is expected,

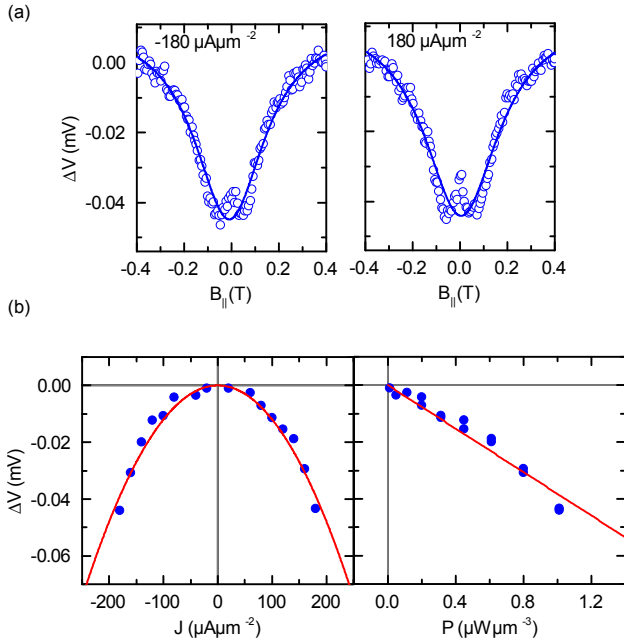


Figure 4. (Color online) **Thermal inverted Hanle effect at room temperature.** (a) Thermally induced spin accumulation in Si, detected as a voltage change (ΔV) employing inverted Hanle effect with in-plane magnetic field. The plot shows the inverted Hanle data for heating currents of $\pm 180 \mu\text{A}\mu\text{m}^{-2}$ in two opposite directions. (b) Left panel: Thermal inverted-Hanle signal ΔV (symbols) versus Joule heating current density, together with a quadratic fit (solid line). Right panel: ΔV (symbols) as a function of Joule heating power, and a linear fit (solid line).

since the Joule heating and therefore the gradient should be independent of current direction. For $T_{Si} > T_{FM}$ a spin polarization identical to the electrical spin injection is observed, which corresponds to majority spin accumulation in the Si. This should be the case for a decaying TSP above E_F as confirmed by our electrical bias dependence measurements presented in Fig. 2d. Figure 3c shows the amplitude of the thermal Hanle signal measured for different Joule heating currents. The amplitude of the thermal spin signal is found to scale quadratically with the heating current density and hence linearly with the applied heating power, which confirms the thermal origin of the Hanle signal¹².

Furthermore, we employ the inverted Hanle effect²⁰ to detect the thermal creation of spin accumulations in Si at room temperature. The local magnetostatic fields arising from interface roughness in a ferromagnetic tunnel contact is known to reduce the spin accumulation in semiconductors. The inverted Hanle effect serves as experimental signature which recovers the reduced spin accumulation by applying an in-plane magnetic field $B_{||}$ ²⁰. Figure 4 shows the measured data due to thermal spin injection for the case of $T_{Si} > T_{FM}$ in the same Co/SiO₂/n-type Si device. An inverted thermal Hanle signal of $\Delta V_{iH} = 45 \mu\text{V}$ could be detected for a current density

of $J = \pm 180 \mu\text{A}\mu\text{m}^{-2}$ (Fig. 4a). As the Joule heating is independent of the current direction, spin signals of same sign and magnitude are obtained for both current directions. Figure 4b shows the amplitude of the inverted thermal Hanle signal for different Joule heating currents, which is also found to scale quadratically with the heating current density and linearly with the applied heating power. This scaling of the spin signal is consistent with a thermally induced spin accumulation in Si¹².

The total magnitude of the thermal spin accumulation in n-type Si is the sum of the Hanle (ΔV_H) and inverted Hanle (ΔV_{iH}) amplitudes²⁰. A total thermal spin signal of $\Delta V = 95 \mu\text{V}$ corresponds to a spin splitting $\Delta\mu = 2\Delta V/TSP = 0.54 \text{ meV}$ ($TSP = 0.35$, assumed for SiO₂/Co contact). This corresponds to an electron spin polarization of 1% in the n-type Si conduction band created by thermal spin injection at room temperature, considering a parabolic conduction band and a Fermi-Dirac distributions for each spin direction ($n \uparrow$ and $n \downarrow$). The magnitude of the thermal spin accumulation defined in terms of a Seebeck spin tunneling coefficient $S_{st} = \Delta\mu/\Delta T$, is found to be 1.08 meV/K . There can be some discrepancy with theory due to inaccuracy in the determination of ΔT , as experimental values for the thermal conductance of different materials and their interfaces are unknown. For the cases of thin tunnel barriers, the interface thermal resistance dominates over the bulk values and also differs with sample preparation conditions. In addition, the ballistic phonon transport and confinement effects in ultra-thin dielectrics and interface roughness play an important role in altering the thermal resistance of the contacts²⁵.

The linear dependence of the spin signal on the heating power confirms the thermal origin of spin accumulation in n-type Si. Furthermore, we can rule out other thermomagnetic effects such as spin related Hall, Nernst, and Ettingshausen effect, because they would not produce the characteristic Lorentzian shape Hanle signal¹². Nevertheless, to rule out all known thermomagnetic effects, measurements at high magnetic fields B_{\perp} were performed. For large enough B_{\perp} the magnetization of the FM rotates out of the plane. This aligns the injected spins parallel to the magnetization direction and produces zero precession, resulting in a recovery of the dephased spin signal. This recovery of the spin signal occurs only if the spin accumulation is produced by a transfer of the spins from the FM. The experimental data for the spin accumulation induced by heating of the Si electrode for $J = \pm 200 \mu\text{A}\mu\text{m}^{-2}$ are shown in Fig. 5. Indeed, the recovery of the spin accumulation is observed when the magnetic field increases above 0.5 T, with the signal saturating at about 2.5 T. This corresponds to the field at which the magnetization of the Co electrode has reached the full out-of-plane orientation^{28,29}. The observation of the high-field recovery of the spin accumulation rules out the spin-Nernst effect and any other mechanism that does not involve transfer of spins from the FM to the Si¹².

In summary, we demonstrate the thermal creation of

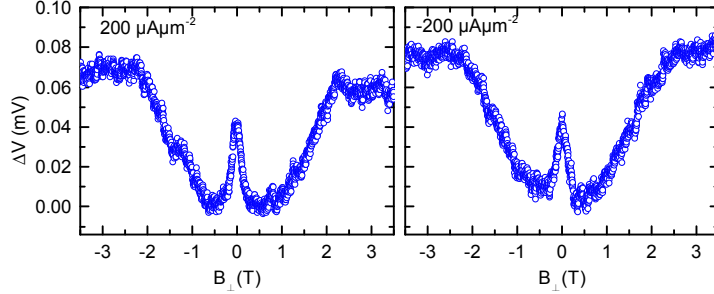


Figure 5. **(Color online)** Detection of thermally induced spin accumulation in Si with perpendicular field up to 3.5 T, for Si heating currents of $\pm 200 \mu\text{A}\mu\text{m}^{-2}$. It shows the rotation and saturation of magnetization of ferromagnetic Co electrode to the out-of-plane direction at higher magnetic fields.

electron spin polarization in n-type Si using the Seebeck spin tunneling mechanism at room temperature. We show that the magnitude of thermally created electron spin polarization scales quadratic with the Joule heating current density and linearly with the heating power. A temperature gradient of few hundred milli kelvins across the ferromagnetic tunnel contacts creates a spin signal of more than $95 \mu\text{V}$, which corresponds to a spin splitting of 0.54 meV and spin polarization of 1% in the conduction band of n-type Si. Furthermore, the control experiment with thermal Hanle measurements at higher magnetic field and the comparison with electrical spin injection experiments rules out any other spurious effects. The advantage of utilizing the Seebeck spin tunneling mechanism is that the magnitude of spin accumulation is not limited to the TSP of ferromagnetic tunnel contact, but can be increased beyond that due to its dependence on energy derivative of TSP . Recently, similar results using MgO tunnel barrier have been reported, during review process of our manuscript³⁰. By carefully designing the interfaces, Seebeck spin tunneling could be useful for creating spin polarizations in non-magnetic materials by itself or together with electrical spin injection, and also for the reusing dissipated heat in electronic devices and circuits.

Acknowledgement: The authors acknowledge the support of colleagues at the Quantum Device Physics Laboratory and Nanofabrication Laboratory at Chalmers University of Technology. We would also like to acknowledge the financial supported from the Nano Area of the Advance program at Chalmers University of Technology, EU FP7 Marie Curie Career Integration grant and the Swedish Research Council (VR) Young Researchers Grant.

REFERENCES

¹G. J. Snyder and E. S. Toberer, *Nat. Mater.* **7**, 105 (2008).

- ²I. Žutić, S. Das Sarma, J. Fabian, and S. D. Sarma, *Rev. Mod. Phys.* **76**, 323 (2004).
- ³A. Fert, *Rev. Mod. Phys.* **80**, 1517 (2008).
- ⁴G. E. W. Bauer, E. Saitoh, and B. J. van Wees, *Nat. Mater.* **11**, 391 (2012).
- ⁵M. Johnson and R. Silsbee, *Phys. Rev. B.* **35**, 4959 (1987).
- ⁶K. Uchida, S. Takahashi, K. Harii, J. Ieda, W. Koshibae, K. Ando, S. Maekawa, and E. Saitoh, *Nature* **455**, 778 (2008).
- ⁷a. Slachter, F. L. Bakker, J.-P. Adam, and B. J. van Wees, *Nat. Phys.* **6**, 879 (2010).
- ⁸M. Hatami, G. Bauer, Q. Zhang, and P. Kelly, *Phys. Rev. Lett.* **99**, 066603 (2007).
- ⁹H. Yu, S. Granville, D. P. Yu, and J.-P. Ansermet, *Phys. Rev. Lett.* **104**, 146601 (2010).
- ¹⁰J. Flipse, F. L. Bakker, a. Slachter, F. K. Dejene, and B. J. van Wees, *Nat. Nanotechnol.* **7**, 166 (2012).
- ¹¹M. Walter, J. Walowski, V. Zbarsky, M. Münzenberg, M. Schäfers, D. Ebke, G. Reiss, A. Thomas, P. Peretzki, M. Seibt, J. S. Moodera, M. Czerner, M. Bachmann, and C. Heiliger, *Nat. Mater.* **10**, 742 (2011).
- ¹²J.-C. Le Breton, S. Sharma, H. Saito, S. Yuasa, and R. Jansen, *Nature* **475**, 82 (2011).
- ¹³R. Jansen, *Nat. Mater.* **11**, 400 (2012).
- ¹⁴R. Jansen, S. P. Dash, S. Sharma, and B. C. Min, *Semicond. Sci. Technol.* **27**, 083001 (2012).
- ¹⁵S. P. Dash, S. Sharma, R. S. Patel, M. P. de Jong, and R. Jansen, *Nature* **462**, 491 (2009).
- ¹⁶R. Jansen, B. C. Min, S. P. Dash, S. Sharma, G. Kioseoglou, A. T. Hanbicki, O. M. J. van 't Erve, P. E. Thompson, and B. T. Jonker, *Phys. Rev. B* **82**, 241305 (2010).
- ¹⁷T. Sasaki, T. Oikawa, T. Suzuki, M. Shiraiishi, Y. Suzuki, and K. Tagami, *Appl. Phys. Express* **2**, 053003 (2009).
- ¹⁸K. Jeon, B. Min, I. Shin, C.-Y. Park, H.-S. Lee, Y. Jo, and S. Shin, *Appl. Phys. Lett.* **98**, 262102 (2011).
- ¹⁹C. H. Li, O. M. J. van 't Erve, and B. T. Jonker, *Nat. Commun.* **2**, 245 (2011).
- ²⁰S. P. Dash, S. Sharma, J.-C. Le Breton, J. Peiro, H. Jaf-

- frès, J.-M. George, A. Lemaître, and R. Jansen, Phys. Rev. B **84**, 054410 (2011).
- ²¹R. Jansen, A. M. Deac, H. Saito, and S. Yuasa, Phys. Rev. B **85**, 1 (2012).
- ²²A. Jain, C. Vergnaud, J. Peiro, J. C. Le Breton, E. Prestat, L. Louahadj, C. Portemont, C. Ducruet, V. Baltz, A. Marty, A. Barski, P. Bayle-Guillemaud, L. Vila, J.-P. Attané, E. Augendre, H. Jaffrès, J.-M. George, and M. Jamet, Appl. Phys. Lett. **101**, 022402 (2012).
- ²³K. Jeon, B. Min, Y. Park, and Y. Jo, Appl. Phys. Lett. (2012).
- ²⁴A. Dankert, R. S. Dulal, and S. P. Dash, Sci. Rep. **3**, 3196 (2013).
- ²⁵T. Yamane, N. Nagai, S.-i. Katayama, and M. Todoki, J. Appl. Phys. **91**, 9772 (2002).
- ²⁶S. Valenzuela, D. J. Monsma, C. Marcus, V. Narayana-murti, and M. Tinkham, Phys. Rev. Lett. **94**, 196601 (2005).
- ²⁷B. G. Park, T. Banerjee, J. Lodder, and R. Jansen, Phys. Rev. Lett. **99**, 23 (2007).
- ²⁸S. Sharma, S. P. Dash, H. Saito, S. Yuasa, B. J. van Wees, and R. Jansen, Phys. Rev. B **86**, 165308 (2012).
- ²⁹S. Sharma, A. Spiesser, S. Dash, S. Iba, S. Watanabe, B. J. van Wees, H. Saito, S. Yuasa, and R. Jansen, Phys. Rev. B **89**, 075301 (2014).
- ³⁰K.-R. Jeon, B.-C. Min, S.-Y. Park, K.-D. Lee, H.-S. Song, Y.-H. Park, and S.-C. Shin, Appl. Phys. Lett. **103**, 142401 (2013).